AMM 2032

The 26th Conference of the Mechanical Engineering Network of Thailand
October 2012, Chiang Rai

The application of semi-discretization method in milling stability with variable pitch and variable helix tool

Satienpong Huyanan[1]

[1] Mahanakorn University of Technology, Bangkok, Thailand, 10530

Abstract

Milling is one of the most versatile metal removal processes in which a rotating cutter removes material of a workpiece. One of limit factors on achieving higher productivity is regenerative chatter arose in cutting processes. Chatter is an unstable cutting condition with excessive vibrations, which leads to a poor surface finish, tool wear and potential damage to the machine or tool. Stability of conventional milling processes are widely studied in the pass decades. Recently, the topic of variable pitch and variable helix milling tools has gained attention as an alternative method to improve stability boundary of the milling processes by altering chatter pattern using irregular setting of a milling cutter. This study presents the application of semi-discretization method on stability analysis of variable pitch and variable helix milling tools.

Keywords*:* Milling, Chatter, Semi-discretization, Variable helix and pitch, Variable time delay.

1. Introduction

Variable pitch and helix milling tools have been studied by recent researches [1-2, 7] as an alternative mean for improving chatter stability. Fig.1 schematically shows a variable pitch and helix milling tool. It can be seen that each axial layer or disk of the tool can have different angles between one tooth and the next. This provides the possibility to avoid chatter occurred by judicious choice of the tool pitch and helix angles. The first analytical method on irregular tooth pitch cutter was introduced by Slavicek [7] as an alternative passive method to improve the stability condition in the milling process, using Tlusty's orthogonal cutting chatter theory [8]. Altintas et al [2] extended their so-called single solution method to predict the stability in variable pitch cutter. Up to date, a few studies were proposed to investigate the effect of higher order harmonics of the cutting forces on stability in such variable pitch cutter. However, in the recent publication, Turner et al [1] described the use of different helix angles on an end-mill to improve stability condition, and stability was predicted using an average helix angle along an axial depth of cut based on the extended method of single frequency solution.

There have been little or no reports of stability models for these classes of milling tool with interrupt cutting at low radial immersion. It transpires that this stability problem is well suited to the semi-discretization method developed by Insperger et al [3-5], which will be extended in this study. This paper will describe the theoretical basic and presents the extended analytic on stability of variable pitch and helix milling tools.

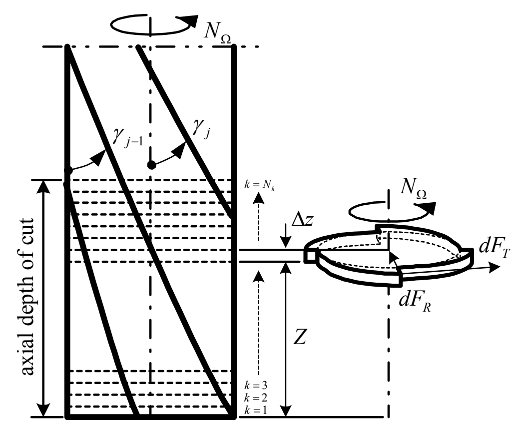

Fig. 1 Variable pitch and helix milling tool.

2. Mechanistic model of cutting forces

The linear orthogonal cutting forces model for the milling process is developed based on an end-mill cutter with a diameter of D, N_z flutes and a constant tooth angle ψ, as shown in Fig.2. The tool is rotated at spindle speed of N_Ω revolution per minute (RPM) and the angular position of the tool is described by $\theta(t)$. At each revolution, the static cutting zone is defined between the entry cutting angle θ_{en} and the exit cutting angle θ_{ex}. The axial depth of cut Z is divided into a differential thickness Δz with N_k stacks such that $Z = \Delta z \cdot N_k$.

The cutting force components, F_X and F_Y, acting on the tool can be described by [9],

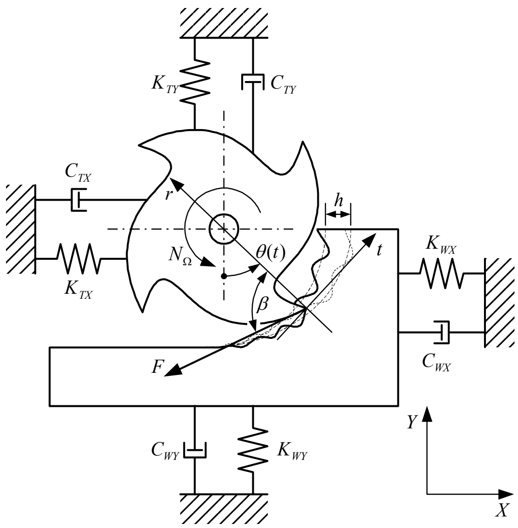

Fig.2 Dynamic model of a milling system

$$\begin{bmatrix} F_X(t) \\ F_Y(t) \end{bmatrix} = \underbrace{\begin{bmatrix} F_{SX} \\ F_{SY} \end{bmatrix}}_{\text{static force}} - \underbrace{\sum_{j=1}^{N_z}\sum_{k=1}^{N_k}\left(\Delta z K_t \mathbf{W}_{j,k}(t)\begin{bmatrix} \Delta x_t - \Delta x_{t-\tau_j} \\ \Delta y_t - \Delta y_{t-\tau_j} \end{bmatrix}\right)}_{\text{regenerative force}} \quad (1)$$

$$\mathbf{W}_{j,k}(t) = g_{j,k}(t)\begin{bmatrix} -s\theta_{j,k}(t) & +c\theta_{j,k}(t) \\ -c\theta_{j,k}(t) & -s\theta_{j,k}(t) \end{bmatrix} \cdot \begin{bmatrix} K_r \cdot s\theta_{j,k}(t) & -K_r \cdot c\theta_{j,k}(t) \\ s\theta_{j,k}(t) & -c\theta_{j,k}(t) \end{bmatrix} \quad (2)$$

*Note: $s\theta = \sin\theta$ and $c\theta = \cos\theta$

Where j refers to the flute number and k denotes index of the infinitesimal disk at axial height z, as shown in Fig.1. K_t and K_r are the specific tangential and radial cutting force coefficients, respectively. $\mathbf{W}_{j,k}(t)$ defines the directional oriented coefficient matrix, which is periodic at tooth passing frequency for the cutter with regular pitch angle, but at spindle frequency for the cutter with variable pitch angle.

Next, the cutting force model is extended to include the effect of different helix angle on each flute j of the end-mill. This can be achieved by introducing the instantaneous angular position $\theta_{j,k}(t)$ of flute j at axial height z as follows,

$$\theta_{j,k}(t) = \theta_0(t) - \psi_j - \frac{2\tan\gamma_j}{D}\cdot z \quad (3)$$

where ψ_j defines the relative angle between the first and j^{th}-flutes. γ_j defines the constant helix angle on flute j. $\theta_0(t)$ is the based angular position of the spindle rotation N_Ω at time t, determined by $\theta_0(t) = N_\Omega \cdot t$ (rad). The cutter is assumed to have a different constant helix angle on each flute, thes the pitch angle $\phi_{j,k}$ of flute j at axial height z is related to the relative angle ψ_j of flute j and $j-1$ as follows,

$$\phi_{j,k} = (\psi_j - \psi_{j-1}) + \frac{2(\tan\gamma_j - \tan\gamma_{j-1})}{D}\cdot z \quad (4)$$

Then, the time delay $\tau_{j,k}$ of flute j at axial height z can be resolved as a function of the pitch angle $\phi_{j,k}$ and the spindle speed N_Ω RPM as the form,

$$\tau_{j,k} = \frac{60 \times \phi_{j,k}}{2\pi \cdot N_Z} \quad (5)$$

It can be seen that, by setting the variable pitch and helix angle on the cutter, the constant time delay of the conventional milling processes will be altered. The system becomes the variable time delay system in comparison to the constant time delay system of the uniform pitch cutter.

Note that, using the different pitch angle $\phi_{j,k}$ will result in a non-constant uncut chip thickness $f_{t,j}$ for each flute of the cutter. Then, Substitute Eq. (3) into the cutting forces model (Eqs. (1) and (2)) yields the total cutting forces over the axial depth of cut Z as follows,

$$\begin{bmatrix} F_X(t) \\ F_Y(t) \end{bmatrix} = \sum_{j=1}^{N_Z}\left\{\int_0^Z g_{j,k}(t)\cdot K_t \cdot \left(\underbrace{\begin{bmatrix} -s\theta_{j,k}(t) & +c\theta_{j,k}(t) \\ -c\theta_{j,k}(t) & -s\theta_{j,k}(t) \end{bmatrix}\cdot\begin{bmatrix} K_r \\ 1 \end{bmatrix}\cdot f_{t,j}\cdot s\theta_{j,k}(t)}_{\text{static cutting force part}} \right.\right.$$
$$\left.\left. - \underbrace{\begin{bmatrix} -s\theta_{j,k}(t) & +c\theta_{j,k}(t) \\ -c\theta_{j,k}(t) & -s\theta_{j,k}(t) \end{bmatrix}\cdot\begin{bmatrix} K_r \cdot s\theta_{j,k}(t) & -K_r\cdot c\theta_{j,k}(t) \\ s\theta_{j,k}(t) & -c\theta_{j,k}(t) \end{bmatrix}\cdot\begin{bmatrix} \Delta x_t - \Delta x_{t-\tau_{j,k}} \\ \Delta y_t - \Delta y_{t-\tau_{j,k}} \end{bmatrix}}_{\text{regenerative cutting force part}} \right)\cdot dz \right\} \quad (6)$$

where $(\Delta x_t, \Delta y_t)^T$ is a relative displacement vector of flute j at height z of the tool-workpiece system and $(\Delta x_{t-\tau_{j,k}}, \Delta y_{t-\tau_{j,k}})^T$ refers to a state vector at time delay $\tau_{j,k}$. Then, defines the static cutting force due to the uncut chip thickness $f_{t,j}$ at time t of flute j as $(F_{SX}, F_{SY})^T$, Eq. (6) can be re-written in a compact form and as,

$$\begin{bmatrix} F_X(t) \\ F_Y(t) \end{bmatrix} = \underbrace{\begin{bmatrix} F_{SX} \\ F_{SY} \end{bmatrix}}_{\text{static cutting force}} - \underbrace{\sum_{k=1}^{N_k} \left\{ \int_0^Z K_t \mathbf{W}_{j,k}(t) \begin{bmatrix} \Delta x_t - \Delta x_{t-\tau_{j,k}} \\ \Delta y_t - \Delta y_{t-\tau_{j,k}} \end{bmatrix} dz \right\}}_{\text{regenerative cutting force}} \tag{7}$$

Where

$$\mathbf{W}_{j,k}(t) = g_{j,k}(t) \begin{bmatrix} -s\theta_{j,k}(t) & +c\theta_{j,k}(t) \\ -c\theta_{j,k}(t) & -s\theta_{j,k}(t) \end{bmatrix} \cdot \begin{bmatrix} K_r \cdot s\theta_{j,k}(t) & -K_r \cdot c\theta_{j,k}(t) \\ s\theta_{j,k}(t) & -c\theta_{j,k}(t) \end{bmatrix} \tag{8}$$

$$g_{j,k}(t) = \begin{cases} 1 & \theta_{en} \le \theta_{j,k}(t) \le \theta_{ex} \\ 0 & \text{otherwise} \end{cases}$$

$\mathbf{W}_{j,k}(t)$ describes the directional oriented coefficient matrix, which is a time-periodic at the spindle rotation frequency for the case of irregular pitch cutters. However, if the cutter has the uniform pitch angle, then $\tau_{j,k}$ will reduce into a constant time delay τ. Hence, $\mathbf{W}_{j,k}(t)$ becomes a periodic at the tooth passing frequency.

Then, the continuous cutting force of Eq. (7) is discretizated by dividing the axial depth of cut Z into N_k elements of a finite axial disk of thickness Δz, such that $Z = N_k \cdot \Delta z$. This results in the discrete cutting force model as,

$$\begin{bmatrix} F_X(t) \\ F_Y(t) \end{bmatrix} = \underbrace{\begin{bmatrix} F_{SX} \\ F_{SY} \end{bmatrix}}_{\text{static cutting force}} - \underbrace{\sum_{j=1}^{N_z} \sum_{k=1}^{N_k} \left(\Delta z K_t \mathbf{W}_{j,k}(t) \begin{bmatrix} \Delta x_t - \Delta x_{t-\tau_{j,k}} \\ \Delta y_t - \Delta y_{t-\tau_{j,k}} \end{bmatrix} \right)}_{\text{regenerative cutting force}} \tag{9}$$

The corresponding variable time delay $\tau_{j,k}$ of the finite axial disk of element k at flute j can be determined by,

$$\phi_{j,k} = (\psi_j - \psi_{j-1}) + \frac{2(\tan\gamma_j - \tan\gamma_{j-1})}{D} \cdot \left(k + \frac{1}{2}\right) \cdot \Delta z \tag{10}$$

$$\tau_{j,k} = \frac{60 \times \phi_{j,k}}{2\pi \cdot N_Z}$$

if the case of a variable pitch end-mill is considered, then $\gamma_j = \gamma_{j-1}$. Thus, $\phi_{j,k}$ becomes $\phi_j = \psi_j - \psi_{j-1}$ and $\tau_{j,k} = \tau_j$. In representing the cutting forces with the discrete form of Eq. (9), itis now applicable to apply the method of semi-discretization to analyze stability problem of the cutting system with variable time delay.

3. Stability analysis in milling with variable time delay

Considering the dynamics of the milling process, the first order state equation of the milling system can be expressed as [9],

$$\dot{\mathbf{q}}_t = \hat{\mathbf{A}} \cdot \mathbf{q}_t - \hat{\mathbf{B}} \sum_{j=1}^{N_z} \sum_{k=1}^{N_k} \left(\Delta z K_t \mathbf{W}_{j,k}(t) \begin{bmatrix} \Delta x_t - \Delta x_{t-\tau_j} \\ \Delta y_t - \Delta y_{t-\tau_j} \end{bmatrix} \right) \tag{11}$$

$$\begin{bmatrix} \Delta x_t \\ \Delta y_t \end{bmatrix} = \hat{\mathbf{C}} \cdot \mathbf{q} \quad \text{and} \quad \begin{bmatrix} \Delta x_{t-\tau_j} \\ \Delta y_{t-\tau_j} \end{bmatrix} = \hat{\mathbf{C}} \cdot \mathbf{q}_{t-\tau_j}$$

where $\mathbf{q}$ is the state vector, which defines the decoupled modal coordinates of the system. $\hat{\mathbf{A}}$, $\hat{\mathbf{B}}$ and $\hat{\mathbf{C}}$ are a modal parameters matrix of the dynamic cutting system, which can be determined using the method of modal testing and analysis techniques. Since the modal parameters of the system are constant, thus $\hat{\mathbf{B}}$ is a constant matrix that can be distributed into the summation and rewritten Eq. (11) as,

$$\dot{\mathbf{q}}_t = \hat{\mathbf{A}} \cdot \mathbf{q}_t - \sum_{j=1}^{N_z} \sum_{k=1}^{N_k} \left(\Delta z K_t \hat{\mathbf{B}} \mathbf{W}_{j,k}(t) \begin{bmatrix} \Delta x_t - \Delta x_{t-\tau_j} \\ \Delta y_t - \Delta y_{t-\tau_j} \end{bmatrix} \right) \tag{12}$$

At the instantaneous time t, the state vector $\mathbf{q}_{t-\tau_j}$ is dependent on flute j and height z of the finite axial disk element as oppose to the state vector $\mathbf{q}_t$, thus only the state vector $\mathbf{q}_t$ can be taken off the summation. Then, decoupling the state vector $(\Delta x_t, \Delta y_t)^T$ of Eq. (12) yields,

$$\dot{\mathbf{q}} = \left\{ \hat{\mathbf{A}} - \sum_{j=1}^{N_z} \sum_{k=1}^{N_k} \left(\Delta z K_t \hat{\mathbf{B}} \mathbf{W}_{j,k}(t) \cdot \hat{\mathbf{C}} \right) \right\} \cdot \mathbf{q} + \sum_{j=1}^{N_z} \sum_{k=1}^{N_k} \left(\Delta z K_t \hat{\mathbf{B}} \mathbf{W}_{j,k}(t) \cdot \hat{\mathbf{C}} \cdot \mathbf{q}_{t-\tau_{j,k}} \right) \tag{13}$$

Since $\mathbf{W}_{j,k}(t)$ is periodic at the spindle rotation N_Ω RPM , the principle period is $T = 60/N_\Omega$. The time period T is divided into p equal intervals with length Δt as shown by the discretization scheme of Fig.3 such that,

$$\Delta t = \frac{T}{p} = \frac{60}{N_\Omega \cdot p} \tag{14}$$

For $t \in [t_j, t_{j+1}]$ and applying the method of single frequency solution, then $\mathbf{W}_{i,j,k}$ becomes an average coefficient over the period T and defined by a constant $\mathbf{W}_{0,j,k}$ as,

$$\mathbf{W}_{0,j,k} = \frac{1}{T} \cdot \int_0^T \mathbf{W}_{j,k}(t) \cdot \mathrm{d}t \tag{15}$$

If the method of convolution integral is adapted, then $\mathbf{W}_{i,j,k}$ is held constant over the i^{th} interval with length Δt such that,

$$\mathbf{W}_{i,j,k} = \frac{1}{\Delta t} \cdot \int_{t_i}^{t_i + \Delta t} \mathbf{W}_{j,k}(t) \cdot \mathrm{d}t \tag{16}$$

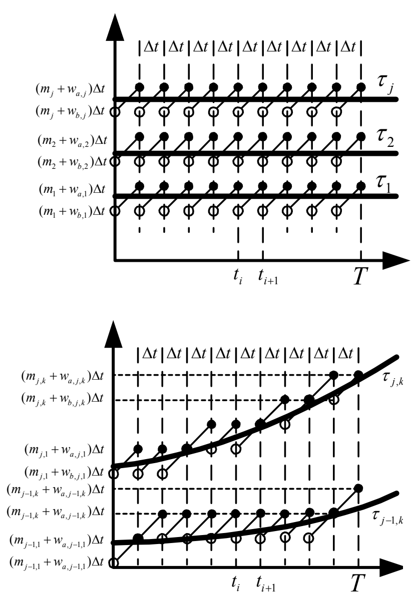

Fig.3 Discretization scheme

Discretization of the delayed term yields the approximated delayed states as,

$$\mathbf{q}(t_i - \tau_{j,k}) \approx \mathbf{q}\left(t_i + \frac{\Delta t}{2} - \tau_{j,k} \right) \approx w_a \, \mathbf{q}_{i-m_{j,k}} + w_b \, \mathbf{q}_{i-m_{j,k}+1} = \mathbf{q}_{\tau_{j,k},i} \tag{17}$$

The delayed index $m_{j,k}$ is defined by relationship between Δt and the delay $\tau_{j,k}$ as,

$$m_{j,k} = \mathrm{fix}\left(\frac{\tau_{j,k}}{\Delta t} + \frac{1}{2} \right) \tag{18}$$

where the weights of $\mathbf{q}_{i-m_{j,k}}$ and $\mathbf{q}_{i-m_{j,k}+1}$ are given by,

$$w_{a,j,k} = \frac{\tau_{j,k}}{\Delta t} - \left(m_{j,k} + \frac{1}{2} \right) \text{ and } w_{b,j,k} = 1 - w_{a,j,k}$$

Substitution of Eqs. (15)-(17) into Eq. (13) over each time interval i of $t \in [t_j, t_{j+1}]$, where $\mathbf{q}(t_i) = \mathbf{q}_{t_i}$. Thus, Eq. (13) can be approximated as,

$$\dot{\mathbf{q}}_{t_i} = \mathbf{A}_i \cdot \mathbf{q}_{t_i} + \sum_{j=1}^{N_z} \sum_{k=1}^{N_k} \left[\mathbf{B}_{i,j,k} \left(w_{a,j,k} \, \mathbf{q}_{i-m_{j,k}+1} + w_{b,j,k} \, \mathbf{q}_{i-m_{j,k}} \right) \right] \tag{19}$$

Where

$$\begin{aligned} \mathbf{A}_i &= \hat{\mathbf{A}} - \sum_{j=1}^{N_z} \sum_{k=1}^{N_k} \left(\Delta z K_t \hat{\mathbf{B}} \mathbf{W}_{i,j,k} \cdot \hat{\mathbf{C}} \right) \\ \mathbf{B}_{i,j,k} &= z K_t \hat{\mathbf{B}} \mathbf{W}_{i,j,k} \cdot \hat{\mathbf{C}} \end{aligned} \tag{20}$$

Since $\mathbf{A}_i$ and $\mathbf{B}_i$ are constant coefficients for $t_i \in [t_i, t_{i+1}]$, the system of Eq. (13) is linearized by the approximating system of Eq. (20) for $t_i \in [t_i, t_{i+1}]$, then the principle of superposition exists. The solution of Eq. (20) for the initial condition $\mathbf{q}(t_i) = \mathbf{q}_i$ reads,

$$\mathbf{q}(t) = e^{\mathbf{A}_i \Delta t} \mathbf{q}_i + \sum_{j=1}^{N_z} \sum_{k=1}^{N_k} \left[\left(e^{\mathbf{A}_i \Delta t} - \mathbf{I} \right) \mathbf{A}_i^{-1} \cdot \mathbf{B}_{i,j,k} \left(w_{a,j,k} \, \mathbf{q}_{i-m_{j,k}+1} + w_{b,j,k} \, \mathbf{q}_{i-m_{j,k}} \right) \right] \tag{21}$$

For time $t = t_{i+1}$, this gives $\mathbf{q}(t) = \mathbf{q}_{i+1}$ and the state $\mathbf{q}_{i+1}$ is given by,

$$\mathbf{q}_{i+1} = \mathbf{P}_i \mathbf{q}_i + \sum_{j=1}^{N_z}\sum_{k=1}^{N_k}\left[\mathbf{Q}_{i,j,k}\left(w_{a,j,k}\,\mathbf{q}_{i-m_{j,k}+1} + w_{b,j,k}\,\mathbf{q}_{i-m_{j,k}}\right)\right] \quad (22)$$

Where

$$\mathbf{P}_i = \exp(\mathbf{A}_i \Delta t)$$
$$\mathbf{Q}_{i,j,k} = [\exp(\mathbf{A}_i \Delta t) - \mathbf{I}]\mathbf{A}_i^{-1}\mathbf{B}_{i,j,k} \quad (23)$$

Since the system of Eq. (13) is variable time delay such that $m_{j,k}$ is not constant, then the finite dimension of the discrete map is determined by the integer $m_{\max}$. If Eq. (13) represents the milling system using the n-dimensional state vector, then the approximated $n(m_{\max}+2)$-dimensional state vector is defined by,

$$\mathbf{q}_i = \left(q_i, \dot{q}_i, q_{i-1}, q_{i-2} \;\cdots\; q_{i-m_{\max}+1}, q_{i-m_{\max}}\right)^T$$

and the discrete map can be constructed as,

$$\mathbf{q}_{i+1} = \mathbf{\Phi}_i \cdot \mathbf{q}_i \quad (24)$$

where each $n(m_{\max}+2)$-dimensional transition matrix $\mathbf{\Phi}_i$ is given by,

$$\mathbf{\Phi}_i = \begin{bmatrix} \mathbf{P}_i & \mathbf{0} & \cdots & \mathbf{0} & \mathbf{0} & \mathbf{0} \\ [\mathbf{I} \;\; \mathbf{0}] & \mathbf{0} & \cdots & \mathbf{0} & \mathbf{0} & \mathbf{0} \\ [\mathbf{0} \;\; \mathbf{0}] & \mathbf{I} & \cdots & \mathbf{0} & \mathbf{0} & \mathbf{0} \\ \vdots & \vdots & \ddots & \vdots & \vdots & \vdots \\ [\mathbf{0} \;\; \mathbf{0}] & \mathbf{0} & \cdots & \mathbf{I} & \mathbf{0} & \mathbf{0} \\ [\mathbf{0} \;\; \mathbf{0}] & \mathbf{0} & \cdots & \mathbf{0} & \mathbf{I} & \mathbf{0} \end{bmatrix} + \sum_{j=1}^{N_Z}\sum_{k=1}^{N_k}\begin{bmatrix} \mathbf{0} & \cdots & \mathbf{0} & \overbrace{w_{a,j,k}\mathbf{Q}_{i,j,k}}^{m_{j,k}-1} & \overbrace{w_{b,j,k}\mathbf{Q}_{i,j,k}}^{m_{j,k}} & \mathbf{0} \\ [\mathbf{0} \;\; \mathbf{0}] & \cdots & \mathbf{0} & \mathbf{0} & \mathbf{0} & \mathbf{0} \\ [\mathbf{0} \;\; \mathbf{0}] & \cdots & \mathbf{0} & \mathbf{0} & \mathbf{0} & \mathbf{0} \\ \vdots & \ddots & \vdots & \vdots & \vdots & \vdots \\ [\mathbf{0} \;\; \mathbf{0}] & \cdots & \mathbf{0} & \mathbf{0} & \mathbf{0} & \mathbf{0} \\ [\mathbf{0} \;\; \mathbf{0}] & \cdots & \mathbf{0} & \mathbf{0} & \mathbf{0} & \mathbf{0} \end{bmatrix} \quad (25)$$

In the case of single frequency approximation, Eq. (25) becomes the delayed transition matrix $\mathbf{\Phi}_T$ since $\mathbf{\Phi}_T$ is constant over all discretization intervals. Alternatively, for applying the method of convolution integral, the delayed Floquet transition matrix $\mathbf{\Phi}_T$ can be obtained by convolution of Eq. (25) over the principle period T for $i = 0,1,\ldots,k-1$, as follows

$$\mathbf{\Phi}_T = \mathbf{\Phi}_{k-1} \cdot \mathbf{\Phi}_{k-2} \cdots \mathbf{\Phi}_1 \cdot \mathbf{\Phi}_0 \quad (26)$$

The $n(m_{\max}+2) \times n(m_{\max}+2)$-dimensional matrix $\mathbf{\Phi}_T$ represents an approximation of the infinite dimensional solution of Eq. (13), and the eigenvalues of $\mathbf{\Phi}_T$ can be used to evaluate stability of Eq. (13). If all eigenvalues of $\mathbf{\Phi}_T$ are within the unit circle, then the system is asymptotically stable. If one of the eigenvalues of $\mathbf{\Phi}_T$ is on the unit circle while the rest are within the unit circle, then the system becomes critically stable. Otherwise, if one of the eigenvalues of $\mathbf{\Phi}_T$ is outside the unit circle, then the system is unstable and thus chatter occurs.

4. Corresponding chatter frequencies

Since stability analysis of Eq. (13) is based on the approximated discrete-time system, it is known that the eigenvalues of the corresponding discrete-time system can be transformed to the eigenvalues of the corresponding continuous-time system [10]. Hence, if φ defines the eigenvalues of the approximated discrete-time system of Eq. (13), then the corresponding eigenvalues λ of the continuous system can be obtained by,

$$\lambda_i = \frac{\ln \varphi_i}{T} = \sigma_i \pm j\omega_i \quad (27)$$

where T denotes a sampling period of the discrete time system, which refers to the principle period at the spindle rotation in this case.

It is clearly seen that frequencies of the system vibrations can be determined according to imaginary part of the eigenvalues λ. However, it is important to note that the transformation from the discrete-time system into the continuous-time system is not unique. This results in accumulation of multipliers of 2π to imaginary part of λ [10].

This allows the corresponding vibration frequencies f_{corr} to be determined as follows,

$$f_{corr} = \left\{\pm\,\omega_i + l\frac{2\pi}{T}\right\} \text{rad/s} = \left\{\pm\frac{\omega_i}{2\pi} + l\frac{N_\Omega}{60}\right\} \text{Hz} \quad (28)$$
$$\text{where } l = \ldots, -1, 0, 1, \ldots$$

If one of $\mathrm{Re}(\lambda_i) = \sigma$ of Eq. (27) is zero, the system becomes critically stable. This results in pure oscillation of the system at corresponding frequency determined from $\mathrm{Im}(\lambda) = \omega$. Since the principle period is larger than the maximum delayed period, three types of instabilities of periodic solutions associated to chatter can possibly occur; a Secondary Hopf-bifurcation, a Period-doubling bifurcation and a Period-one bifurcation. Its corresponding chatter frequencies are listed in Table. 1 [9].

Table. 1 Corresponding chatter frequencies

Type of bifurcation	Correspondent chatter frequencies
Secondary Hopf	$\pm\frac{\omega_i}{2\pi}+l\frac{N_\Omega}{60}$ Hz
Period-doubling	$\left(\frac{1}{2}+l\right)\frac{N_\Omega}{60}$ Hz
Period-one	$0+l\frac{N_\Omega}{60}$ Hz

5. Stability prediction, case studies

The proposed semi-discretization method for the milling process with variable time delay has been evaluated by reconsidering the stability in milling with a variable pitch cutter. Altintas et al [2] presented both numerical and experimental data on the stability analysis of a milling process with variable pitch cutters. This was based on the method of modified single frequency solution, where the evaluation of stability was performed by scanning all possible chatter frequencies and chatter vibration wavelengths.

In [2], the case of a variable pitch milling was investigated using a 2-directional milling system with the dynamics parameters listed in Table. 2. The tool parameters used in the study were: a 4-flutes cutter having diameter 19.05 mm with variable pitch angle of $70°-110°-70°-110°$ and helix angle of $30°$. Cutting tests were conducted on Al-7075 specimens at feed rate 0.0508 mm/tooth with the specific cutting coefficients: $K_t = 697\times10^6$ N/m^2 and $K_r = 0.367$.

Table. 2 Dynamic parameters of the milling cutter

Direction	Mode	ω_n [Hz]	ζ [%]	Residue
x	1st 2nd 3rd	443.62 563.55 778.52	2.86 5.58 5.90	0.08989 0.6673 0.07655
y	1st	516.27	2.50	0.834

To apply the semi-discretization method in this study, first, the first-order state equation describing the 2-directional milling system was constructed and then substituted into Eq. (13). Since the varying pitch angle on the cutter is repeated for every 2-flutes, $\mathbf{W}_{j,k}(t)$ is a periodic function with the principle period T at the rate of half the spindle speed N_Ω, thus $T = 60/(N_\Omega/2)$. Then, discretization of T into p intervals, such that $T = p\cdot\Delta t$. In this study, discretization of the principle period was chosen for $p = 50$ in order to preserve computational time. The delayed Floquet transition matrix $\mathbf{\Phi}_T$ is then numerically evaluated over specific range of spindle speeds and depths of cut using the Matlab programming. The analysis was done on both the methods of single frequency approximation (doted-line) and the convolution integral method (solid-line), as shown in Fig. 4.

For a variable pitch cutter with constant helix angle, the time delay can be determined by the angle between two subsequence teeth. The varying delay for given spindle speed is defined by $60\times[70°-110°-70°-110°]/(360°\times N_\Omega)$ seconds, which results in the DDE system with two constant time delays. The approximated delayed terms can be obtained using Eqs. (18) and (19) where the maximum delay index describes a finite dimension of the approximated discrete delayed system. Then, the local stability for the given axial depth of cut Z can be determined by evaluation of the eigenvalues of the constructed delayed transition matrix $\mathbf{\Phi}$ as defined by Eqs. (21)-(26). Finally, the stability charts are obtained by iterating the stability analysis over a set of spindle speeds and axial depths of cut.

The stability charts for the variable pitch cutter are presented for half immersion operations as shown in Fig.4(a) for the stability results obtained using the extended method of single frequency solution and Fig.4(b) for the semi-discretization method. In the frequency diagram, dash-doted lines denote harmonics of the principle period of the system and the dashed lines denote the structural natural frequency. It can be seen that both the stability charts predict almost the same stability results apart from the unstable period-one and period-doubling bifurcations presented in the semi-discretization method. The boundary of these unstable period-one and period-doubling types are not significant since only small part of the stability region are cut off. It can be seen in the frequency diagram that the unstable period-one bifurcation is expected if the corresponding chatter frequencies cross harmonics of the principle period while the unstable period-doubling bifurcation occurs if the corresponding chatter frequencies intersect each other. However, the routes of instability for the unstable period doubling are separated quickly after it passes through -1 on the real axis.

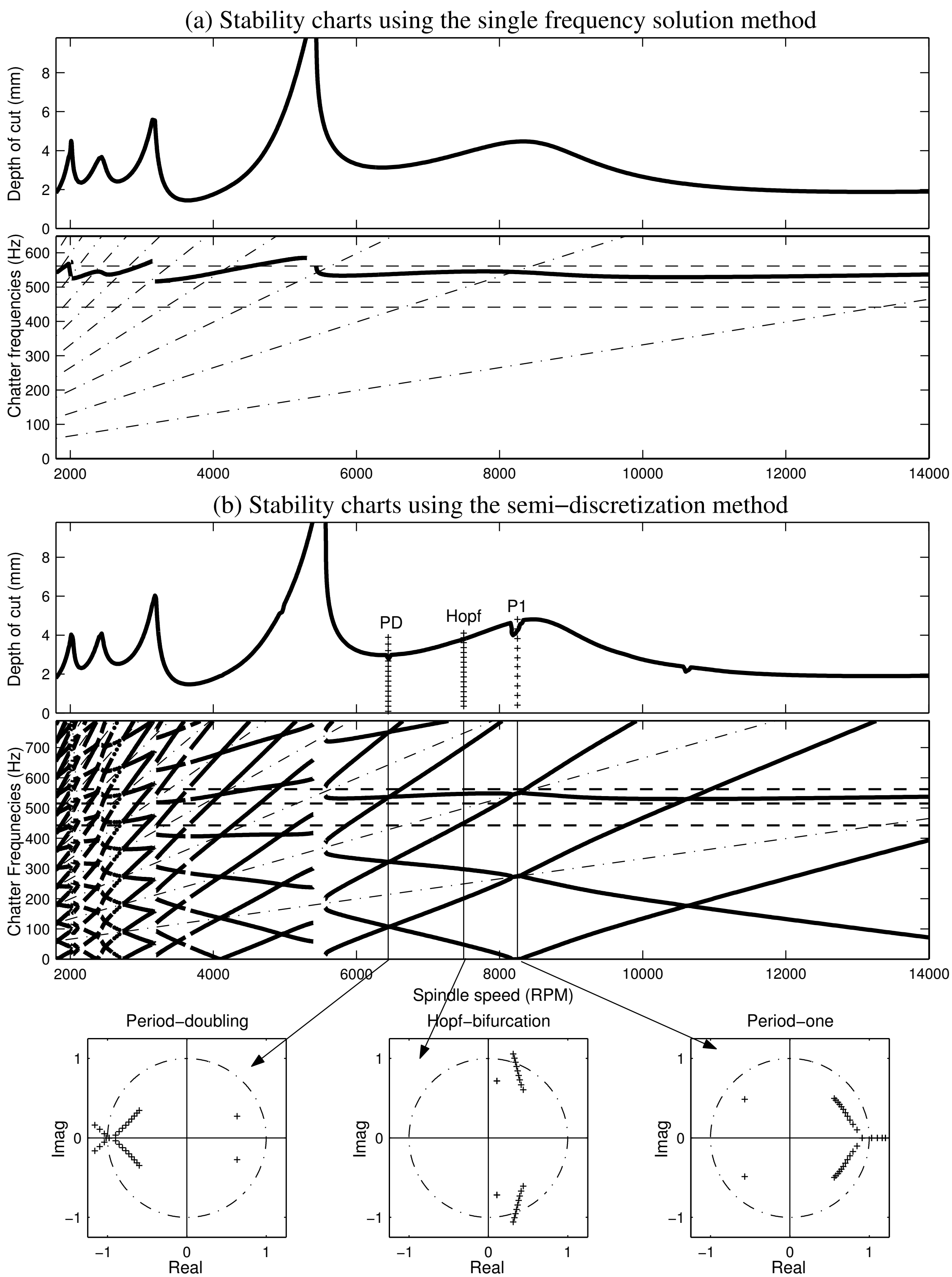

Fig.4 Stability charts for the variable pitch end-mill

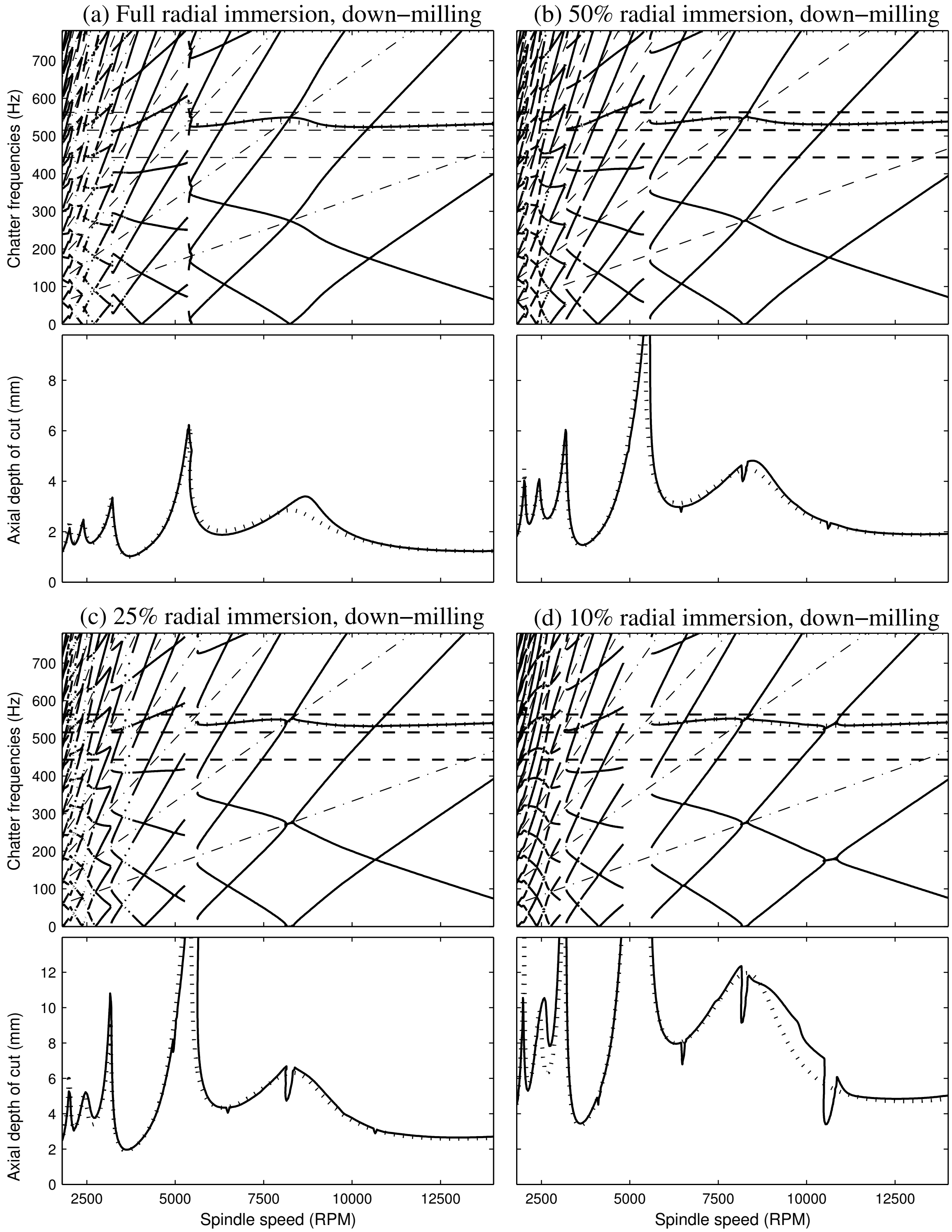

Fig.5 Stability charts for the variable pitch end mill at different radial immersions

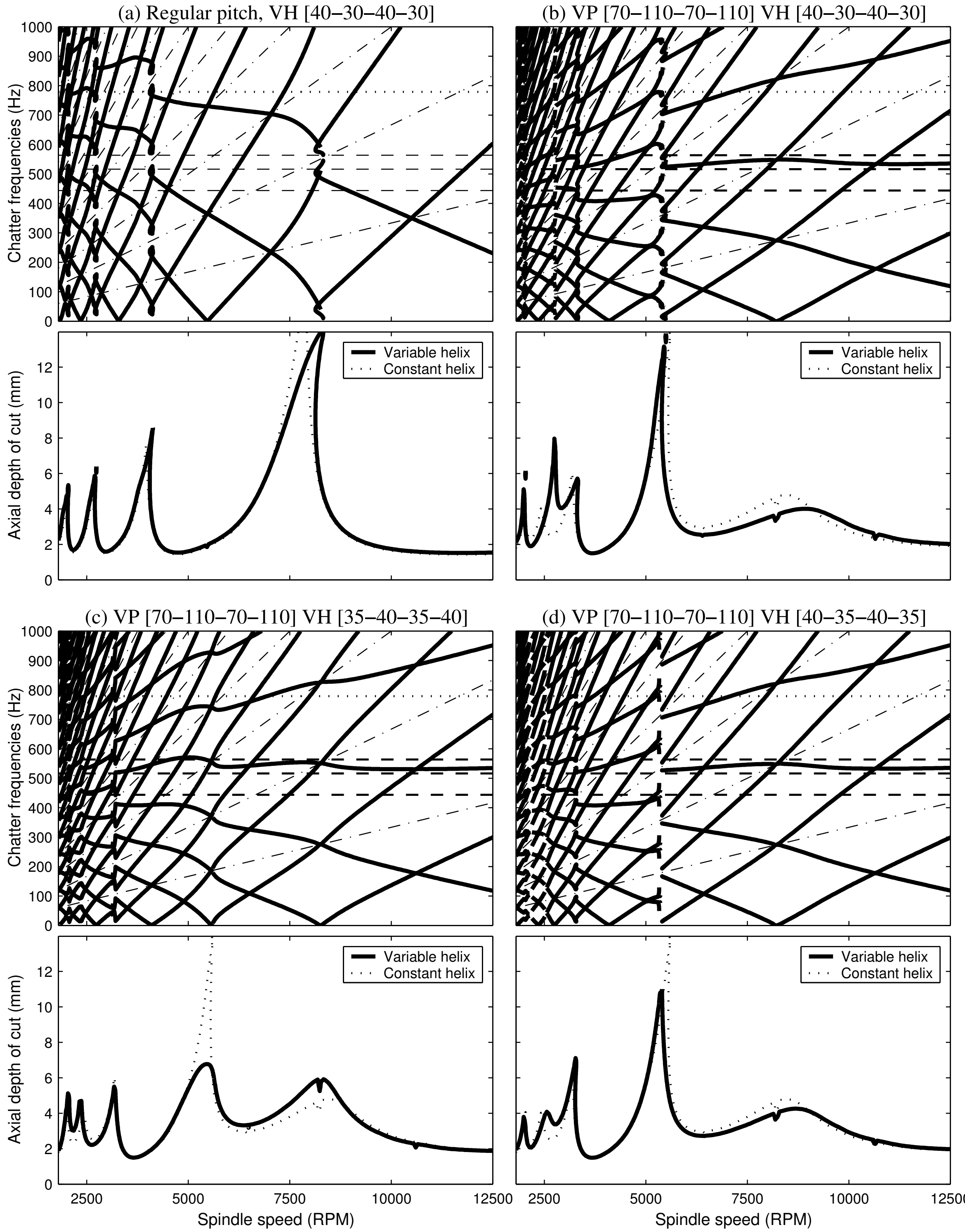

Fig.6 charts for the end mill with varying pitch and helix angles

It can be seen that all the three types of instability occur which can be illustrated by the characteristic multipliers pass through the unit circle in the complex plane. These routes to instabilities are illustrated in the bottom graphs of Fig.4(b) with the corresponding spindle speed and axial depths of cut shown in the stability chart. It can be noticed that an abrupt jump of the characteristic multipliers occurs on all types of instability. This type of eigenvalue discontinuity can be attributed to the fact that the delayed transition matrix $\mathbf{\Phi}$ is asymmetric [6] due to the effect of two constants time delay of the system. It can be seen from the frequency diagram that the spindle speed that pass through or locate in the vicinity of the chatter frequency lines should be avoid in milling with this cutter since large amplitude vibration may occur due to the unstable period-one bifurcation.

Fig.5 presents comparison of the stability charts at different radial immersions. These stability charts were constructed to investigate if the effect of the unstable period-one and period-doubling will be significant on low immersion cutting with the variable pitch cutter. It can be seen that the method of extended single frequency solution can provide almost identical stability results to the convolution integration method, except unstable period-one and period-doubling bifurcation as mentioned above. This suggests that the single frequency solution method is effective to predict the stability boundary.

Next, the analysis was applied to investigate the problem of the cutter with variable helix angles using the similar set of the structural dynamic parameters. First, the stability chart for the cutter with regular pitch angle and varying helix angle of $[40-30-40-30]$ was determined with the semi-discretization method and compared to that of the standard cutter (dotted line) as shown in Fig.6(a). It can be seen that different helix angle on each cutter tooth has significantly no effect on the stability limit but it tends to re-locate the stable pocket region. Then, the stability charts for the variable pitch end mill with three different sets of varying helix angles are shown in Fig.6(b) for a varying helix angles of $[40-30-40-30]$, Fig.6 (c) for a varying helix angles of $[40-35-40-35]$ and Fig.6(d) for a varying helix angles of $[35-40-35-40]$. Again, the analytical stability prediction of the cutter with variable helix angle indicated no difference on the limited axial depth of cut in comparison to one obtained from the variable helix cutter (dotted line) and the effect of varying time delay due to varying helix angle can be observed in the stable pocket region. Result of particular interest is that the spindle speeds where the unstable period-one and period-doubling occurred remain unchanged for all of the sets of varying helix angles.

It is worth discussing that on varying helix angles, one of the limit factors in implementing different helix angle on each flute is the cutter geometry. Since two subsequent teeth are not parallel, this results in the intersection of two subsequent flutes at a axial position Z_l. Thus, flute length of the cutter becomes shorter and constricts the chip exit. This can be presented by a simple trigonometric calculation to obtain the maximum flute length on the cutter with two different helix angles. If two subsequent flutes j and $j-1$ were set with different helix angle as defined by γ_j and γ_{j-1}, respectively. For $\gamma_j > \gamma_{j-1}$, the maximum flute length $h_{l,j}$ of flute j for a cutter of a diameter D can be obtained using the following formula,

$$h_{l,j} = \frac{D \cdot \phi_j}{2\left(\tan\gamma_j - \tan\gamma_{j-1}\right)}$$

where ϕ_j is the angle between flutes j and $j-1$. For a 19.05 mm standard 4-flutes end mill with helix angles of $40°$ and $30°$, the maximum flute length is 57.16 mm. Thus, the effective flute length can be shorter than the maximum length by a factor of 2.

5. Summary

It has been showed in this paper that the semi-discretization method is capable of evaluating the stability in the milling process with variable time delays. First, the stability problem for variable pitch end milling operations was demonstrated. The stability results from two approximations of the time-periodic coefficients show almost no difference in the stability boundary apart from that the unstable period-one and period-doubling behaviour can occur on the stability boundary using the convolution integral method. Then, the example analysis on various types of end mill was carried out. The results indicated that varying helix angles has no effect on the limited axial depth of cut but tends to change the boundary curves.

One of the major disadvantages using the convolution integral method is the computational time to generate the stability charts is tremendous. However, such this study on stability of milling processes with varying time delay is a non-linear analysis, thus the computational time consumed were not the main focus. It has been observed that in most cases, the single frequency solution approximation with discretization of the delayed terms can predict similar stability results to that of the convolution integral method, except the cases concern unstable period-one and period-doubling bifurcation. Hence, the method of single frequency approximation of time-periodic coefficients is suggested if the computational time is a major factor.

Considering the tool geometry in this study, varying helix angles shown little effect in comparison with varying pitch angles. However, further work is recommended to investigate the performance for different types of milling cutter geometries. One of limit factors on implementing a cutter with varying helix angles is the cutter geometry. The large difference between two helix angles setup can result in a shorter flute length, especially on a small diameter end mill.

6. Acknowledgement

The author would like to thank the Department of Mechanical Engineering, University of Sheffield for useful documents and research opportunity.

7. References

7.1 Article in Journals

[1] Turner, S., et al., Modelling of the stability of variable helix end mills, International Journal of Machine Tools and Manufacture, 2007. 47(9): p. 1410-1416.

[2] Altintas, Y., S. Engin, and E. Budak, Analytical Stability Prediction and Design of Variable Pitch Cutters, Journal of Manufacturing Science and Engineering, 1999. 121: p. 173-178.

[3] Insperger, T., et al., Stability of up-milling and down-milling, Part 1: Alternative analytical methods. International Journal of Machine Tools and Manufacture, 2003. 43(1): p. 25-34.

[4] Insperger, T., et al., Multiple chatter frequencies in milling processes. Journal of Sound and Vibration, 2003. 262(2): p. 333-345.

[5] Insperger, T. and G. Stépán, Updated semi-discretization method for periodic delay-differential equations with discrete delay. International Journal of Numerical Methods in Engineering, 2004. 61(1): p. 117-141.

[6] Mann, B.P., et al., Milling Bifurcations from Structural Asymmetry and Nonlinear Regeneration, Nonlinear Dynamics, 2005. 42(4): p. 319-337.

7.2 Proceedings

[7] Slavicek, J. The Effect of Irregular Tooth Pitch on Stability of Milling. in Proceeding of the 6th MTDR Conference. 1965. London: Pergamon Press.

[8] Tlusty, J. and M. Polacek. Stability of Machine Tools Against Self-Excited Vibration in Machining. in Proceedings of the International research in production engineering. 1963. Pittsburgh.

7.3 Books and Thesis

[9] Huyanan, S., An Active Vibration Absorber for Chatter Reduction in Machining, Ph.D. Thesis in Mechanical Engineering 2007, University of Sheffield: Sheffield.

[10] Juang, J.-N. and M. Pan, Identification and Control of Mechanical Systems, ed. 12001, Cambridge, ISBN: 9780521783552, Cambridge University Press.